


ORIGINAL ARTICLE

Proteomics and phosphoproteomics reveal key regulators associated with cytostatic effect of amino acid transporter LAT1 inhibitor

Hiroki Okanishi¹ | Ryuichi Ohgaki^{1,2} | Suguru Okuda¹ | Hitoshi Endou³ |
Yoshikatsu Kanai^{1,2} 

¹Department of Bio-system Pharmacology, Graduate School of Medicine, Osaka University, Osaka, Japan

²Integrated Frontier Research for Medical Science Division, Institute for Open and Transdisciplinary Research Initiative (OTRI), Osaka University, Osaka, Japan

³J-Pharma Co., Ltd., Yokohama, Japan

Correspondence

Yoshikatsu Kanai, 2-2 Yamadaoka, Suita, Osaka 565-0871, Japan.
Email: ykanai@pharma1.med.osaka-u.ac.jp

Funding information

Japan Society for the Promotion of Science, Grant/Award Number: 19K16743, 19H03407 and 18K19429; Japan Agency for Medical Research and Development; Project for Cancer Research And Therapeutic Evolution, Grant/Award Number: JP19cm0106151 and JP20cm0106151; J-Pharma Co., Ltd.

Abstract

L-type amino acid transporter 1 (LAT1) is highly expressed in various cancers and plays important roles not only in the amino acid uptake necessary for cancer growth but also in cellular signaling. Recent research studies have reported anticancer effects of LAT1 inhibitors and demonstrated their potential for cancer therapy. Here, we characterized the proteome and phosphoproteome in LAT1-inhibited cancer cells. We used JPH203, a selective LAT1 inhibitor, and performed tandem mass tag-based quantitative proteomics and phosphoproteomics on four biliary tract cancer cell lines sensitive to JPH203. Our analysis identified hundreds to thousands of differentially expressed proteins and phosphorylated sites, demonstrating the broad influence of LAT1 inhibition. Our findings showed various functional pathways altered by LAT1 inhibition, and provided possible regulators and key kinases in LAT1-inhibited cells. Comparison of these changes among cell lines provides insights into general pathways and regulators associated with LAT1 inhibition and particularly suggests the importance of cell cycle-related pathways and kinases. Moreover, we evaluated the anticancer effects of the combinations of JPH203 with cell cycle-related kinase inhibitors and demonstrated their potential for cancer therapy. This is the first study providing the proteome-wide scope of both protein expression and phosphorylation signaling perturbed by LAT1 inhibition in cancer cells.

KEYWORDS

amino acid transporter system, cell cycle, drug combinations, neoplasms, proteomics

Abbreviations: BCH, 2-amino-2-norbornanecarboxylic acid; BTC, biliary tract cancer; FBS, fetal bovine serum; IMAC, immobilized metal affinity chromatography; IPA, Ingenuity Pathway Analysis; KSEA, kinase-substrate enrichment analysis; LAT1, L-type amino acid transporter 1; LC-MS/MS, liquid chromatography-tandem mass spectrometry; PBS, phosphate-buffered saline; PTS, phase transfer surfactant; TBS, tris-buffered saline; TFA, trifluoroacetic acid; TMT, tandem mass tag.

This is an open access article under the terms of the Creative Commons Attribution-NonCommercial License, which permits use, distribution and reproduction in any medium, provided the original work is properly cited and is not used for commercial purposes.

© 2020 The Authors. *Cancer Science* published by John Wiley & Sons Australia, Ltd on behalf of Japanese Cancer Association.

1 | INTRODUCTION

Dysregulation of amino acid metabolism is an emerging hallmark of cancer-associated metabolic changes.^{1,2} In rapidly proliferating cells such as cancer cells, the synthesis of biological macromolecules such as proteins, nucleic acids, and lipids heavily depends on the uptake of extracellular amino acids to fulfill the massive demand of nutrients.³ Amino acids, not just nutrients, also function as signaling molecules involved in various cellular processes such as cell proliferation, cell survival, and cancer progression.⁴⁻⁷ Transporters which take up extracellular amino acids are commonly upregulated in cancer cells and contribute to the rapid growth and continuous proliferation.^{4,8} L-type amino acid transporter 1 (LAT1), one of the system L amino acid transporters,^{9,10} mediates the uptake of aromatic and branched-chain amino acids (e.g., leucine) in exchange for intracellular amino acids such as glutamine and is highly expressed in various types of cancers but scarcely expressed in normal tissues.¹¹⁻¹⁸ LAT1 controls amino acid balance in cancers cooperating with other amino acid transporters.^{19,20}

In cancer cells, LAT1 plays important roles not only in providing amino acids essential for biomolecule synthesis but also in regulating cellular signaling.^{4,8} A major LAT1 substrate, leucine, stimulates mechanistic target of rapamycin kinase complex 1 (mTORC1) which controls a broad range of cellular processes.²¹ Furthermore, other LAT1 substrate amino acids were also reported to be involved in cellular signaling.⁴ Recent studies have indicated the link between LAT1 and mTORC1 signaling²²⁻²⁴ as well as other signaling pathways^{25,26} in cancer cells. Many studies have reported the anticancer effects induced by LAT1 inhibition in various cancer types.^{22-24,27-33} These findings suggest the importance of LAT1 in cancer biology and its clinical potential as a therapeutic target in cancer treatments.

Recently, several lines of studies have exploited LAT1 for clinical applications such as cancer-specific positron emission tomography,^{34,35} a diagnostic and prognostic marker of cancer,^{32,36-41} and a targeted therapy for cancer treatment.^{4,8,42} A classic system L inhibitor, 2-amino-2-norbornanecarboxylic acid (BCH), inhibits LAT1, and suppresses cancer cell proliferation.^{43,44} Recently, a first-in-class LAT1-specific inhibitor, JPH203 (also called KYT-0353), has been developed.^{27,45} JPH203 shows an anticancer effect against various types of cancers: biliary tract cancer (BTC),³⁰ colon cancer,²⁷ oral cancer,²⁸ T-cell lymphoblastic lymphoma/T-cell acute lymphoblastic leukemia,²² thymic carcinoma,^{23,29} medulloblastoma,²⁴ thyroid cancer,³¹ renal cell carcinoma,³² and bladder carcinoma.³³ A first-in-human phase I clinical trial of JPH203 has already been completed with some promising activity against BTC.⁴⁶ This accumulated evidence suggests the potential of LAT1 as a target for cancer therapy. However, it remains unclear what signaling pathways mediate the effects of LAT1 inhibition and what proteins contribute to an anticancer effect caused by LAT1 inhibition. It is, therefore, important to investigate an anticancer effect of LAT1 inhibitors on a system-wide scale. Recent deep phosphoproteomics arose as advanced tools for the study of cancer therapies using tyrosine kinase inhibitors.⁴⁷ A more recent study showed that phosphoproteomics integrated with global proteomics

revealed key networks of cancer cell resistance to cisplatin,⁴⁸ which shows usefulness of integrative proteomics and phosphoproteomics for the study of anticancer drugs other than kinase inhibitors.

In this study, we conducted global proteomics and phosphoproteomics on cancer cells treated with JPH203. We used immobilized metal affinity chromatography (IMAC) for phosphopeptide enrichment and liquid chromatography–tandem mass spectrometry (LC-MS/MS) with MS2-based quantitation of tandem mass tag (TMT) to characterize the changes in both protein expression and phosphorylation induced by LAT1 inhibition in four BTC cell lines sensitive to JPH203. Our present study revealed biological pathways associated with LAT1 inhibition, and showed regulators and responsible kinases which may function in the downstream of LAT1. In particular, both proteomics and phosphoproteomics implied the significance of cell cycle regulator molecules, especially CDK1 and CDK2, in LAT1-inhibited cells. Furthermore, we evaluated the combinations of JPH203 with cell cycle-related kinase inhibitors and demonstrated their therapeutic potential in cancer treatment.

2 | MATERIALS AND METHODS

2.1 | Cell culture

RPMI-1640 was purchased from Sigma-Aldrich, fetal bovine serum (FBS) from Gibco (Thermo Fisher Scientific), and penicillin/streptomycin from Nacalai Tesque. Human BTC cell lines, HuCCT1 (JCRB0425), KKKU-055 (JCRB1551), KKKU-100 (JCRB1568), and KKKU-213 (JCRB1557), were provided by the Japanese Collection of Research Bioresources. The cells were cultured in RPMI-1640 supplemented with 10% FBS and penicillin/streptomycin at 37°C with 5% CO₂.

2.2 | Preparation of JPH203-treated samples and tryptic digests

Detailed procedures are given in Document S1. In short, the cells were seeded at optimized density depending on the cell lines. Twenty-four hours after the seeding of cells, the medium was changed with the fresh medium with or without 30 μmol/L JPH203. Trypan blue exclusion assay showed the treatment of cells with JPH203 at this concentration did not cause cell death (Figure S1). After 24 hours culture, the cells were washed with ice-cold phosphate-buffered saline (PBS) and harvested. Proteomics sample preparation was conducted using a modified phase transfer surfactant (PTS)-aided digestion strategy.⁴⁹ In short, the cell pellet was lysed in 100 mmol/L Tris (pH 8.5) containing 12 mmol/L sodium deoxycholate, 12 mmol/L sodium N-lauroylsarcosinate, and PhosSTOP by heating. The extracted proteins were reduced with 5 mmol/L dithiothreitol and then alkylated with 10 mmol/L iodoacetamide. After quenching with additional 5 mmol/L dithiothreitol and fivefold dilution with 50 mmol/L ammonium bicarbonate buffer, the proteins were digested with lysyl endopeptidase and were further digested

with trypsin until the digestion was complete. Finally, the resultant solution was desalted by a Sep-Pak Plus C₁₈ cartridge (Waters), followed by lyophilization.

2.3 | Phosphopeptide enrichment using IMAC

Phosphopeptides were enriched from tryptic digests by IMAC as previously described.⁵⁰ Detailed procedures are given in Document S1. In short, we made immobilized Fe(III) affinity chromatography (Fe(III)-IMAC) resin from ProBond nickel-chelating resin (Invitrogen, Thermo Fisher Scientific). Ni²⁺ ion was released from the resin with 50 mmol/L EDTA, pH 8.0. After equilibration with 1% acetic acid, Fe³⁺ ion was chelated to the resin with 100 mmol/L FeCl₃ in 0.1% acetic acid. The resultant Fe(III) IMAC resin was equilibrated with 0.1% TFA/60% acetonitrile. Then, tryptic peptides in 0.1% TFA/60% acetonitrile were loaded to the resin. The resin was washed with 0.1% TFA/60% acetonitrile and subsequently washed with 0.1% TFA. Then, the enriched phosphopeptides were eluted with 1% phosphoric acid.

2.4 | TMT labeling of tryptic peptides and enriched phosphopeptides

Each of tryptic digests (10 µg) for global proteomics and phosphopeptides for phosphoproteomics was desalted by C18 StageTip method⁵¹ using 3M Empore C18 disk (GL Science) and dried up. The dried samples were labeled with TMT 10-plex isobaric label reagent (Thermo Fisher Scientific) according to the manufacturer's protocol. Detailed procedures are given in Document S1.

2.5 | High pH C18 reversed-phase fractionation

For quantitative proteomics, 2 µg of TMT-labeled tryptic digests of JPH203-treated and nontreated control samples (n = 3) were mixed and subjected to high-pH C18 StageTip fractionation by sequential elution of peptides with 25 mmol/L ammonium formate (pH 10.0) containing 5%, 7%, 9%, 11%, 13%, 15%, 17.5%, 20%, 22.5%, 25%, 27%, and 50% acetonitrile. For quantitative phosphoproteomics, TMT-labeled phosphopeptides were mixed and subjected to C18 StageTip fractionation by sequential elution of peptides with 25 mmol/L ammonium formate (pH 10.0) containing 5%, 7%, 9%, 11%, 13%, 15%, 17.5%, 20%, and 50% acetonitrile. All fractions were dried up and dissolved in 0.1% TFA.

2.6 | LC-MS/MS analysis, data analysis, and in silico analysis

The peptides of each sample were separated on a nano HPLC system. The eluted peptides were analyzed with a Q-Exactive orbitrap

mass spectrometer (Thermo Fisher Scientific), and MS and MS/MS spectral data were acquired. Proteins and phosphopeptides were identified with threshold *q*-value of .01 by analyzing MS and MS/MS data using Proteome Discoverer 2.3 software (Thermo Fisher Scientific). Following the previous study of quantitative proteomics by quantitation at the MS/MS level using TMT,⁵² a *P*-value cutoff and effect size cutoff were used to define differentially expressed proteins and phosphorylated sites as follows: *P*-value < .05 and fold change ≥ 1.2.

Differentially expressed proteins and phosphorylated sites as a result of JPH203 treatment were analyzed by Ingenuity Pathway Analysis (IPA; QIAGEN) to detect activated and inactivated pathways and to predict upstream regulators. Differentially phosphorylated sites were analyzed by kinase-substrate enrichment analysis (KSEA)⁵³ using online tool (<https://casecpb.shinyapps.io/ksea/>)⁵⁴ with PhosphoSitePlus kinase-substrate database. Detailed setting of LC-MS/MS, data analysis, and in silico analysis are given in Document S1.

2.7 | Western blotting

Protein of each sample (10 µg) was separated by SDS-PAGE and transferred to a polyvinylidene difluoride membrane. The membrane was blocked with tris-buffered saline (TBS) containing 0.1% Tween-20 and 5% skim milk, followed by incubation with specific antibodies overnight in TBS containing 0.1% Tween-20 and 1% skim milk. After washing with TBS containing 0.3% Tween-20, the membrane was incubated for 1 hour with secondary antibodies conjugated with horseradish peroxidase in TBS containing 0.1% Tween-20 and 1% skim milk. After washing with TBS containing 0.3% Tween-20, the bands were visualized by chemiluminescence using ECL Prime Western Blotting Detection Reagent (GE Healthcare). Information about the antibodies and their dilutions is given in Document S1.

2.8 | Cell growth inhibition assay

Detailed procedures are given in Document S1. In short, the cells were cultured for 24 hours in the culture medium. The cells were, then, treated with the inhibitors at the indicated concentration in the culture medium. After 3 days treatment, the cell growth was assessed by Cell Counting Kit-8 (Dojindo). The IC₅₀ value was calculated by SigmaPlot 13.0 (Systat Software).

2.9 | Cell cycle assay

Detailed procedures are given in Document S1. In short, the BTC cells were treated with 30 µmol/L JPH203 for 24 hours in the same way as in proteomics sample preparation. The cell cycle distributions were assessed by Muse Cell Cycle kit (Merck Millipore) following the manufacturer's instruction.

3 | RESULTS

3.1 | Identification of proteome and phosphoproteome in LAT1-inhibited and control BTC cells

To investigate anticancer effects caused by the inhibition of LAT1, we conducted the integrated proteomics and phosphoproteomics and examined the global changes in protein expression and phosphorylation induced by the treatment with a selective LAT1 inhibitor, JPH203, which exerts a cytostatic effect. Because the phase I clinical trial suggested that LAT1 inhibition by JPH203 could have a clinical benefit for the treatment of patients with BTC,⁴⁶ we focused on BTC in the present study, and selected four BTC cell lines (KKU-055, KKU-100, KKU-213, and HuCCT1). We first tested the effects of JPH203 on the growth of these cell lines and found that JPH203 inhibited cell proliferation of all four cell lines in a concentration-dependent manner with IC_{50} values 0.94, 3.75, 7.77, and 1.29 $\mu\text{mol/L}$ for KKU-055, KKU-100, KKU-213, and HuCCT1, respectively (Figure 1).

To reveal the antiproliferation effect of JPH203, we conducted global proteomics and phosphoproteomics on these BTC cells treated with JPH203 for 24 hours and on the control nontreated cells (Figure 2). Trypsin digestion peptides and phosphopeptides enriched by IMAC were fractionated by high pH C18 StageTip, respectively, followed by LC-MS/MS with MS2-based TMT quantification.

In the global proteomics, we identified an average of 54 106 nonredundant peptides belonging to an average of 6431 proteins. In the phosphoproteomics, an average of 21 340 phosphopeptides were identified. MS2-based TMT quantification approaches provided an average of 4983 quantifiable proteins (Table S2). An average of 20 278 quantifiable phosphopeptides (Table S3) and an average of 15 019 quantifiable phosphorylation sites (Table S4) were also obtained. Figure 3A and Figure S2 show good reproducibility

among biological replicates of quantifiable proteins and phosphorylation sites.

3.2 | Identification of differentially expressed proteins and differentially phosphorylated sites in LAT1-inhibited cells

The differentially expressed proteins and differentially phosphorylated sites between JPH203-treated and control cells were identified in four BTC cell lines (Figure 3B and Figure S3). We found differentially expressed proteins as follows: 348, 342, 252, and 1315 proteins in KKU-055, KKU-100, KKU-213, and HuCCT1, respectively. We also found differentially phosphorylated sites: 4777, 3943, 3990, and 5574 sites in KKU-055, KKU-100, KKU-213, and HuCCT1, respectively.

To validate the changes of phosphorylation found in our phosphoproteomics, we selected four differentially phosphorylated sites (Ser-939 of TSC2, Ser-241 of PDK1, Thr-202/Tyr-204 of Erk1/2, and Thr-180/Tyr-182 of p38 MAPK). Western blot confirmed the changes of phosphorylation on all of these sites (Figure S4).

The expression of amino acid transporters is altered according to amino acid availability.¹⁰ Because LAT1 transports various amino acids,^{9,10} LAT1 inhibition could influence the expression of multiple amino acid transporters. Among 60 recognized amino acid transporters in human genome,¹⁰ our proteomics identified 14, 15, 16, and 11 transporters in KKU-055, KKU-100, KKU-213, and HuCCT1, respectively (Figure S5). Of these identified amino acid transporters, we found 4, 6, 7, and 3 transporters were upregulated by JPH203 treatment in KKU-055, KKU-100, KKU-213, and HuCCT1, respectively. No amino acid transporters were downregulated by JPH203. It is notable that seven amino acid transporters were commonly upregulated in at least two different cell lines: LAT1, 4F2hc, xCT, ASCT1, ASCT2, SNAT1, and SNAT2. The observed upregulation of LAT1 and 4F2hc by JPH203 was consistent with previous report,^{24,30} which supports our proteome-wide quantification results.

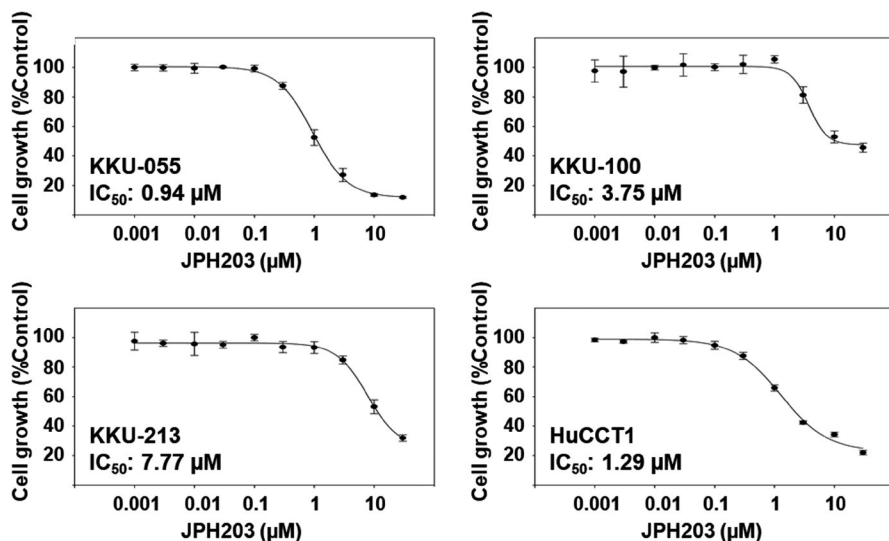


FIGURE 1 Growth inhibition of biliary tract cancer (BTC) cells by JPH203. JPH203 suppressed the proliferation of BTC cells in a concentration-dependent manner with IC_{50} values indicated in the figure

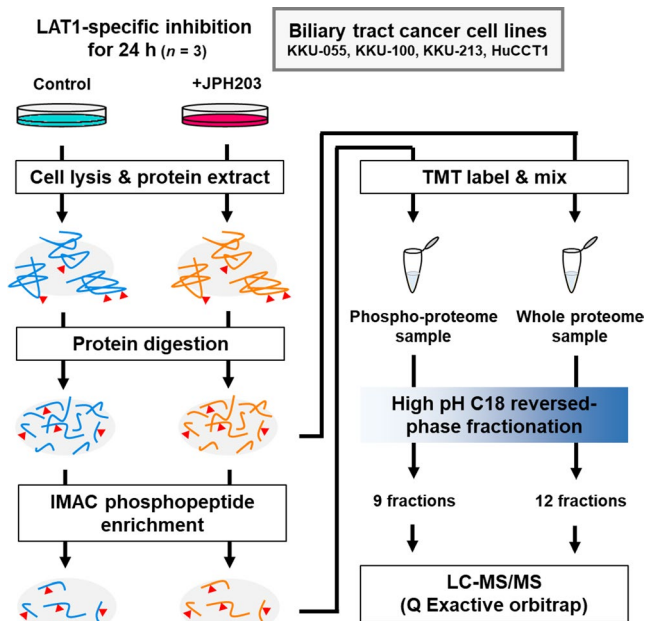


FIGURE 2 Workflow of quantitative proteomics and phosphoproteomics to study the effects of L-type amino acid transporter 1 (LAT1) inhibition in biliary tract cancer (BTC) cell lines. Tryptic peptide samples were prepared from the cells treated with 30 $\mu\text{mol/L}$ JPH203 for 24 h and the control nontreated cells ($n = 3$). For phosphoproteomics, phosphopeptides were enriched by immobilized metal affinity chromatography (IMAC). After labeled with tandem mass tag (TMT) reagent and mixed, peptide and phosphopeptide samples were subject to high pH C18 fractionation, respectively. All fractions were analyzed by Q Exactive mass spectrometer

3.3 | Pathway analysis of differentially expressed proteins and phosphorylated sites

To specify what cellular functions were altered by LAT1 inhibition, we assessed the functional roles of differentially expressed proteins by pathway analysis. The differentially expressed proteins were mapped to cellular pathways in each cell line using IPA. Among activated and inactivated pathways (Table S5), we focused on the pathways commonly activated or inactivated in at least two cell lines to describe cellular responses generally detected in LAT1-inhibited cells (Figure 4A). Interestingly, we found two “cell cycle pathways” belonging to such a category. “G2/M DNA damage checkpoint regulation pathway” was activated in three cell lines, and “Mitotic roles of Polo-like kinase pathway” was inactivated in two cell lines. These two pathways include CCNB1, PLK1, CDK1, CDC20, CKS1B, AURKA, KIF11, KIF23, and PRC1 as differentially expressed proteins (Table S6, and Figure S6A,B). These results suggest that LAT1 inhibition induces cell growth arrest, which was consistent with our cell proliferation assay (Figure 1). We also found activation of “tRNA charging” in three cell lines (Figure 4A), which includes aminoacyl-tRNA synthetases such as AARS, CARS, GARS, SARS, and WARS as differentially expressed proteins (Table S6, and Figure S6C).

We also conducted pathway analysis on the proteins with differentially phosphorylated sites using IPA. Among activated and inactivated pathways (Table S5), we focused on the pathways commonly activated or inactivated in at least two cell lines (Figure 4B). It is notable that four signaling pathways in the category of “Actin cytoskeleton regulatory pathways” were activated: “Actin cytoskeleton signaling,” “Paxillin signaling,” “Ephrin receptor signaling,” and “Cdc42 signaling.” In these pathways, JPH203 treatment caused the changes of phosphorylation of proteins such as serine/threonine protein kinase (PAK1, PAK2, ROCK1, ROCK2, MAPK14, CDC42BPA), tyrosine protein kinase (PTK2, ABL1), cell adhesion-related proteins (PXN, TLN1, TLN2, VCL), actin filament regulatory proteins (WASL, ACTN1, DIAPH3, MYH9, FNBP1L), signal transduction-associated proteins (PIK3C2A, SHC1, ABI1), guanine nucleotide exchange factor (VAV2, ARHGEF12, TRIO, NGEF), which control actin cytoskeleton dynamics, cell motility, and adhesion (Table S7 and Figure S7A-D). Furthermore, the activation of “ERK/MAPK signaling” and “SAPK/JNK signaling” were also detected in two cell lines (Figure 4B, Table S5, and Figure S7E,F).

3.4 | Upstream regulator analyses of differentially expressed proteins and differentially phosphorylated sites

To obtain clues to key regulators involved in anticancer effects of LAT1 inhibition, we conducted analysis of upstream regulators which could induce changes in protein expression. Upstream regulator analysis of differentially expressed proteins showed hundreds of possible regulators (Table S8). Of these, 85 regulators were commonly activated or inhibited in at least two cell lines (Table S9). We further assigned them to functional groups (Figure 5A). Among the 85 common regulators, 25 were assigned to a “transcription regulator” group. In this group, activating transcription factor 4 (ATF4), cyclin-dependent kinase inhibitor 2A (CDKN2A), zinc finger and BTB domain-containing protein 17 (ZBTB17), and nuclear protein 1 (NUPR1) were suggested to be activated in all four cell lines. The possible activation of lysine-specific demethylase 5B (KDM5B) and tumor suppressor p53 (TP53) were found among three cell lines. In contrast, the following factors were shown to be possible inactivated regulators in all four cell lines: cyclin D1 (CCND1), transcriptional coactivator YAP1 (YAP1), microphthalmia-associated transcription factor (MITF), and T-box transcription factor TBX2 (TBX2). The inactivation of forkhead box protein M1 (FOXM1), mediator of RNA polymerase II transcription subunit 1 (MED1), and transcription factor E2F2 (E2F2) were suggested among three cell lines. Furthermore, we found five regulators in a “kinase” group and nine regulators in a “growth factor, receptor, and cytokine” group: the inactivation of estrogen receptor (ESR1) and prostaglandin E2 receptor EP2 subtype (PTGER2) in all four cell lines, the activation of eIF-2-alpha kinase GCN2 (EIF2AK4) and transcription factor E2F1 (E2F), and the inactivation of receptor tyrosine-protein kinase erbB-2 (ERBB2) and

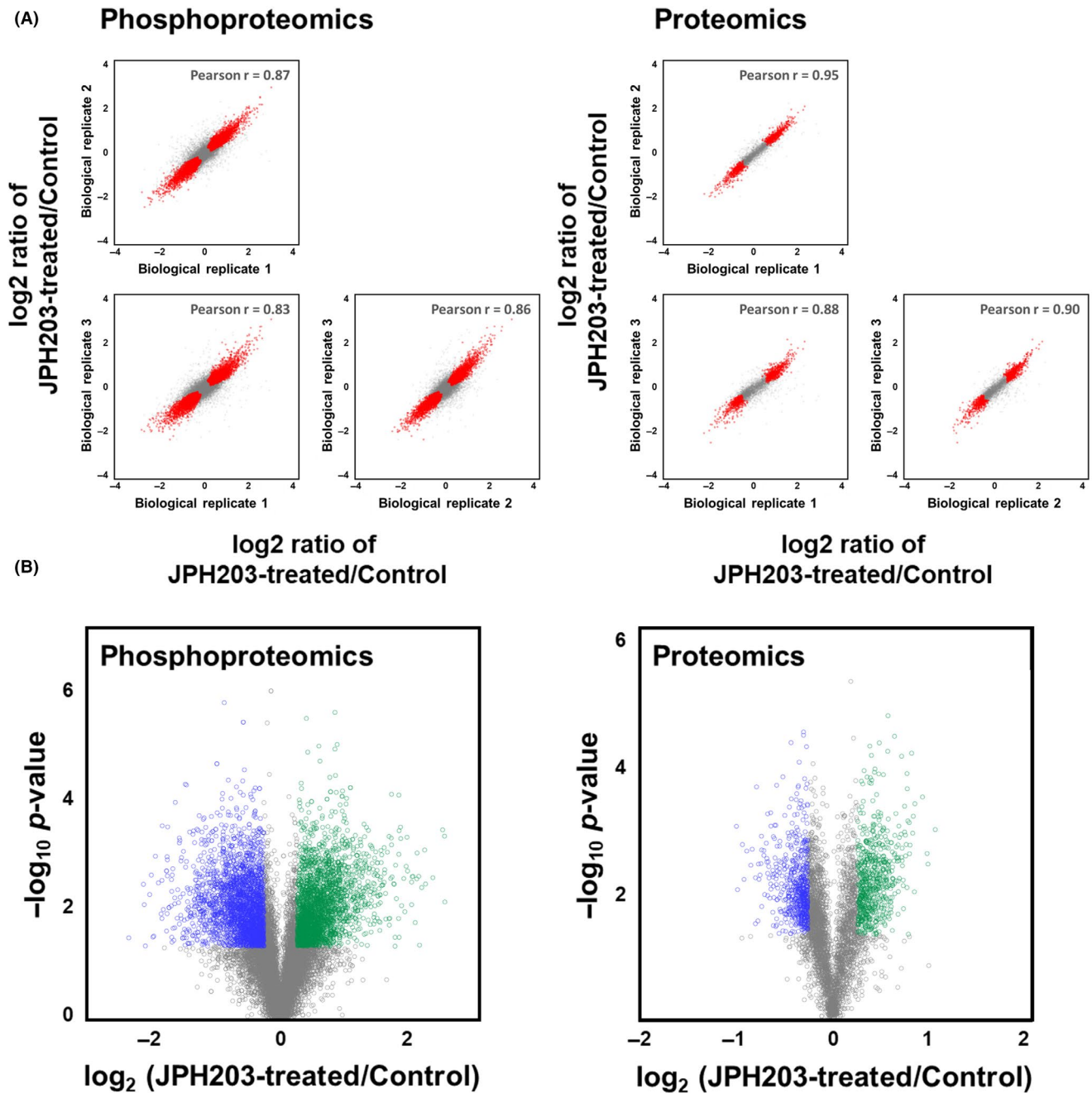


FIGURE 3 Reproducibility between biological replicates and the changes of protein expression and phosphorylation caused by L-type amino acid transporter 1 (LAT1) inhibition in proteomics and phosphoproteomics conducted on HuCCT1 as a representative. A, Representative scatter plots showing log₂ fold changes of proteome and phosphoproteome between biological replicates of JPH203-treated/control samples. Plots of differentially expressed proteins and phosphorylated sites are shown in red. B, Representation of quantitative proteomics and phosphoproteomics data from JPH203-treated and control samples. A volcano plot was generated by plotting $-\log_{10} P$ -values against log₂ fold changes of relative abundance ratio between JPH203-treated and control samples. Plots of differentially expressed proteins and phosphorylated sites are shown in green and blue

tribbles homolog 3 (TRIB3) in three cell lines. We also found five regulators in a “microRNA” group such as activation of let-7 in all four cell lines and mir-21 in three cell lines.

We also conducted upstream regulator analysis of differentially phosphorylated sites (Table S8). Among the upstream regulators, we found 12 regulators commonly activated or inhibited by LAT1

inhibition with JPH203 in at least two cell lines (Table S9) and assigned them to functional groups (Figure 5B). Of these 12 common regulators, six were assigned to a “kinase” group. In this group, the possible inactivation of cyclin-dependent kinase 1 and 2 (CDK1 and CDK2; Figure 5C,D), cyclin B1 (CCNB1), and cyclin E1 (CCNE1) were found, which are cell cycle-related proteins.

FIGURE 4 Heatmap showing activated and inactivated pathways induced by L-type amino acid transporter 1 (LAT1) inhibition, which were commonly detected in at least two cell lines. Activation z-scores of activated or inactivated pathways from proteomics (A) and phosphoproteomics (B) in KKKU-055, KKKU-100, KKKU-213, and HuCCT1 are shown by Ingenuity Pathway Analysis (IPA)

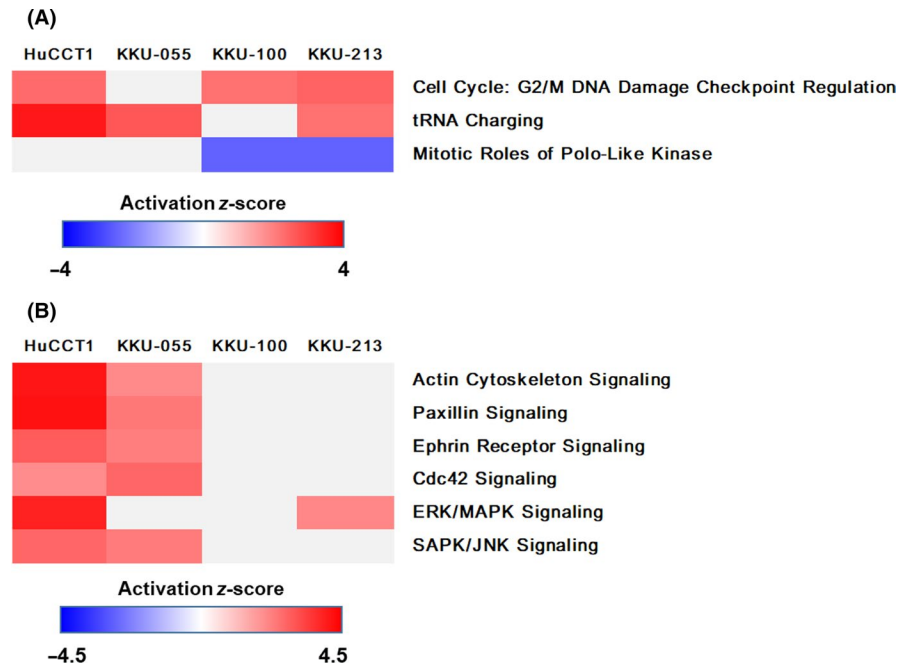
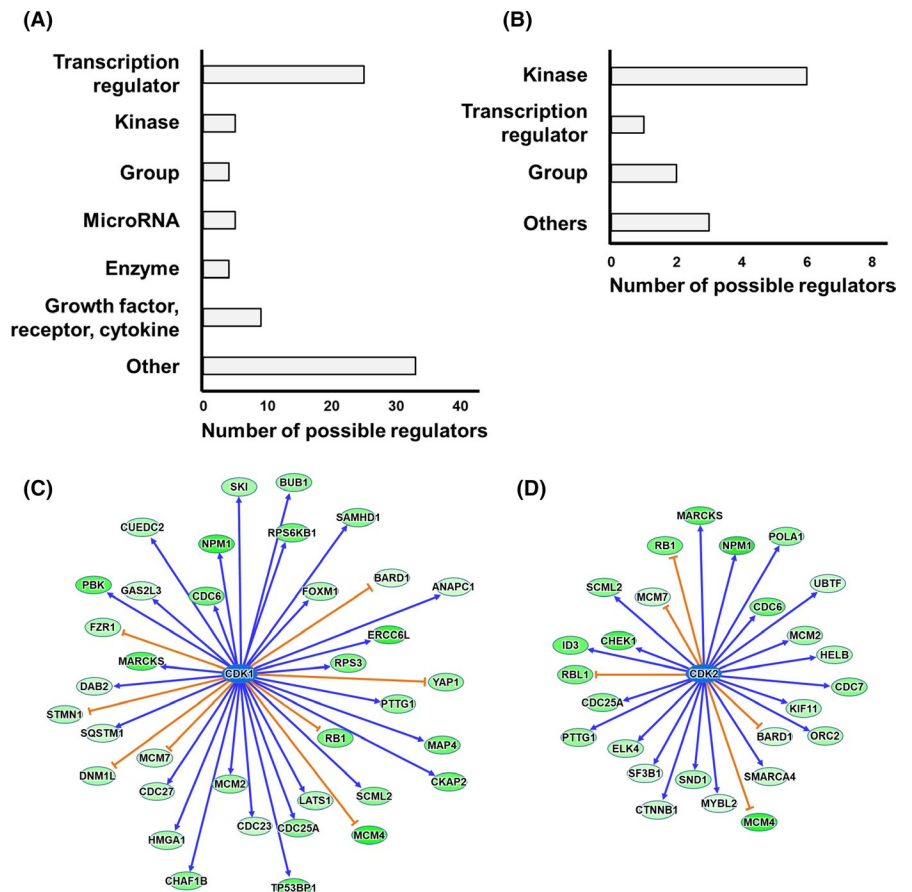


FIGURE 5 Distributions of the functional groups of possible regulators associated with L-type amino acid transporter 1 (LAT1) inhibition, which were commonly detected in at least two cell lines. The upstream regulators were predicted from proteomics (A) and phosphoproteomics (B) by Ingenuity Pathway Analysis (IPA). Network models depicting the interaction between CDKs (CDK1 [C] and CDK2 [D]) and their substrates. Networks in KKKU-055 are shown as representatives. Proteins with decreased phosphorylation are shown with green circles



3.5 | Kinase-substrate enrichment analysis of differentially phosphorylated sites in LAT1 inhibition

To further investigate signaling pathways affected by LAT1 inhibition, we analyzed the differentially phosphorylated sites by KSEA,

which let us estimate the activity of kinases based on the global phosphorylation changes in reference to the database of kinase-substrate relationships.⁵³ As a result, we found a subset of kinases whose activities may be influenced by LAT1 inhibition as follows: 13, 10, 9, and 16 kinases in KKKU-055, KKKU-100, KKKU-213, and HuCCT1,

respectively (Table S10). Among them, seven kinases were suggested to be commonly inactivated by JPH203 treatment in different cell lines (Figure 6A). Interestingly, of these seven kinases, CDK1, CDK2, CDK3, CDK4, CDK6, and aurora kinase A (AURKA) are cell cycle-related kinases. Notably, the inactivation of CDK1 and CDK2 was suggested in all four cell lines. On the other hand, four kinases were suggested to be commonly activated by JPH203 treatment in different cell lines (Figure 6A).

3.6 | Validation of decreased phosphorylation of CDK1/CDK2 substrate proteins

It was notable that KSEA suggested the inactivation of CDK1 and CDK2 by JPH203 treatment in all four cell lines (Figure 6A). To validate

phosphorylation changes of CDK1/CDK2 substrates shown in KSEA, we selected the sites with phosphorylation decreased in all four cell lines: Ser-54 of Cdc6, Ser-807/811 of Rb, and Ser-1213 of TOP2A, which are cell cycle-related proteins listed as substrates of CDK1 and CDK2 in PhosphoSitePlus kinase-substrate database used for KSEA. Western blot confirmed that the phosphorylation of these sites was decreased by JPH203 treatment, except for TOP2A of KKU-055 which was not detectable (Figure 6B). Because the phosphorylation of these sites has been reported to be involved in the progression of cell cycle,⁵⁵⁻⁶¹ the decreased phosphorylation of these sites may lead to the growth suppression of cancer cells. To reveal whether JPH203 induces cell cycle arrest, we performed cell cycle assay by flow cytometric analysis. Treatment of BTC cells with 30 $\mu\text{mol/L}$ JPH203 for 24 hours resulted in a significant increase of G0/G1 phase, and a significant decrease of S phase and G2/M phase (Figure 6C).

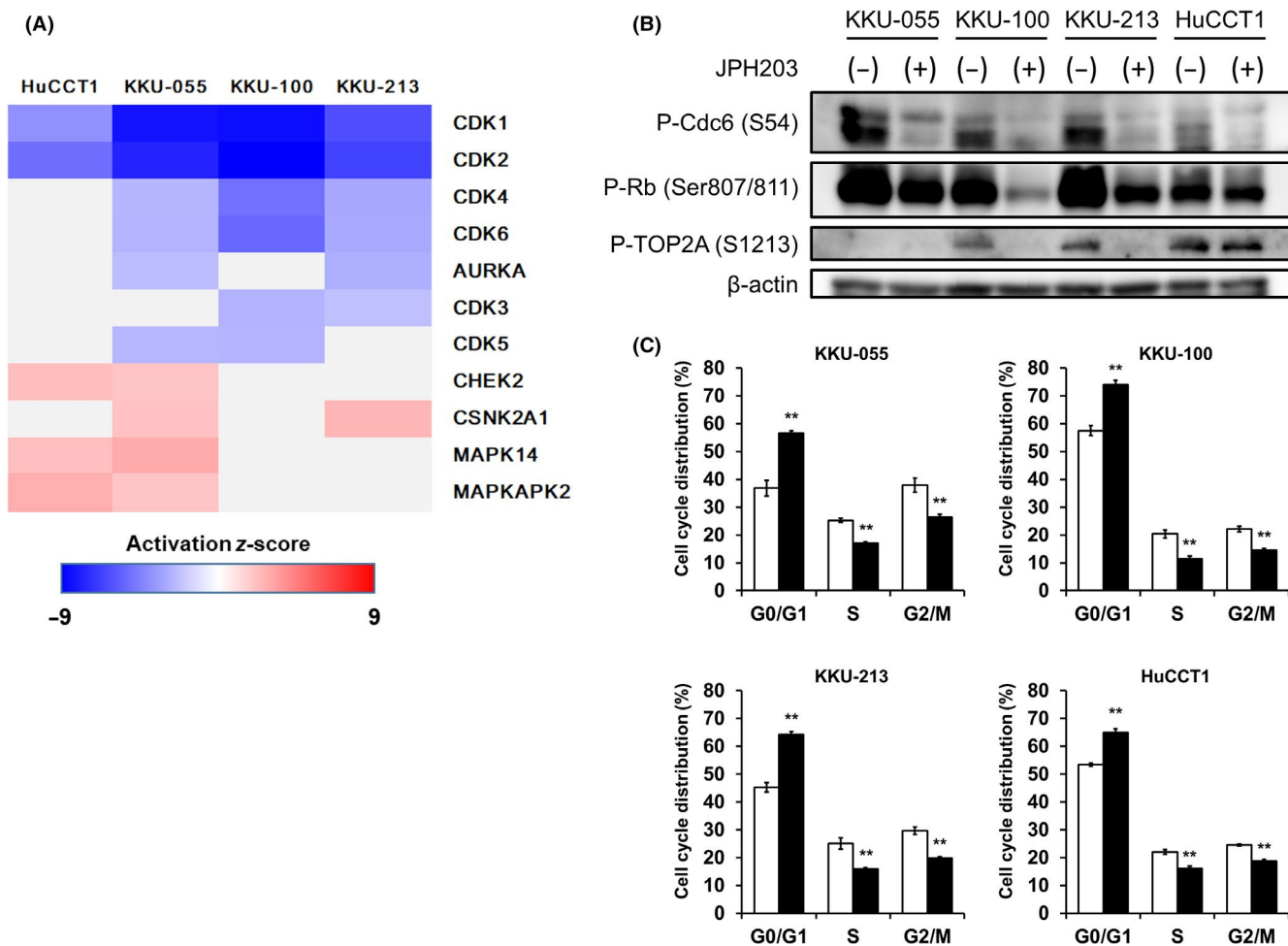


FIGURE 6 Activated and inactivated kinases associated with L-type amino acid transporter 1 (LAT1) inhibition. A, Heatmap showing activation and inactivation z-scores of kinases associated with LAT1 inhibition calculated from phosphoproteomics by kinase-substrate enrichment analysis (KSEA). B, Validation of phosphorylation changes of CDK1/CDK2 substrate proteins in Western blot. The alteration of the phosphorylation associated with LAT1 inhibition was confirmed for the differentially phosphorylated sites found in phosphoproteomics: Ser-54 of Cdc6, Ser-807/811 of Rb, and Ser-1213 of TOP2A. C, Estimation of cell cycle distribution of biliary tract cancer (BTC) cell lines treated with JPH203. Cell cycle distributions of JPH203-treated and control samples are indicated as black and white bars, respectively. Data represent means \pm SD ($n = 3$). ** P -value $< .01$

3.7 | Evaluation of an antiproliferation effect by the combination of JPH203 with cell cycle-related kinase inhibitors

Both proteomics and phosphoproteomics suggested that LAT1 inhibition could influence cell cycle and that the cell cycle-related kinases could be key regulators associated with LAT1 inhibition (Figures 4A, 5A and 6). We, therefore, proposed that targeting cell cycle-related pathways could enhance the anticancer effect caused by LAT1 inhibition and evaluated the combination of JPH203 with the inhibitors of cell cycle-related kinases. Because KSEA suggested common inactivation of six cell cycle-related kinases associated with LAT1 inhibition (Figure 6A), we focused on these kinases as targets: CDK1, CDK2, CDK3, CDK4, CDK6, and AURKA. We examined the effect of commonly used CDK inhibitors (dinaciclib, milciclib, AT7519, and palbociclib) and an aurora kinase inhibitor (alisertib), which cover the entire selectivity range of all the targeted kinases (Table S11). As results, the combination of JPH203 with dinaciclib or AT7519 significantly reduced the proliferation of all four BTC cell lines compared with JPH203 or the kinase inhibitor alone (Figure 7). In addition, the combination of JPH203 with alisertib significantly reduced the proliferation of three cell lines compared with JPH203 or alisertib alone. Milciclib and palbociclib in combination with JPH203 also reduced the proliferation of two cell lines compared with each inhibitor alone.

Moreover, we investigated the potential of cell cycle-related kinase inhibitors in combination with other LAT1 inhibitors. We examined the combination of dinaciclib with BCH, a well-characterized inhibitor of amino acid transporters including LAT1.⁹ This combination significantly reduced cell proliferation compared with each inhibitor alone in all four BTC cell lines (Figure S8). In addition, we also tested the effect of the combination of JPH203 and dinaciclib on cancer other than BTC and found that the combination also significantly reduced cell proliferation compared with JPH203 or dinaciclib alone in a pancreatic cancer cell line, MIA PaCa-2 (Figure S9).

4 | DISCUSSION

Our present study demonstrated the drastic changes of proteome and phosphoproteome associated with LAT1 inhibition. In the BTC cell lines sensitive to JPH203, a specific LAT1 inhibitor, we revealed the global changes in protein expression and phosphorylation by LAT1 inhibition using JPH203. This is the first proteomics and phosphoproteomics study describing the complex influences of LAT1 inhibition on cancer cell biology. Our study also showed common biological pathways and signaling cascades affected by LAT1 inhibition in different cell lines (Figure 4). As cell proliferation of four BTC cell lines was commonly inhibited by JPH203 treatment (Figure 1), these common pathways suggest the key pathways inducing the growth arrests caused by LAT1 inhibition.

Both of our proteomics and phosphoproteomics illustrate the influence of LAT1 inhibition on cell cycle. Recent studies reported that

LAT1 inhibition with JPH203 causes cell cycle arrest through the alteration of CDK4 and CDK6 expression.^{30,31} In our study, proteomics showed that expression of proteins associated with cell cycle was altered in LAT1-inhibited BTC cells. In addition, our phosphoproteomics revealed cell cycle-related kinases and proteins as possible regulators inactivated by LAT1 inhibition (Figure 5). These results are consistent with previous studies.^{30,31} However, in contrast to previous reports, our present study demonstrated CDK1 and CDK2 as possible regulators in LAT1-inhibited cells. In accordance with this observation, LAT1 inhibition decreased the phosphorylation of substrates of cell cycle-related kinases such as CDKs (Figure 6). Such kinases include not only CDK4 and CDK6 but also CDK1, CDK2, CDK3, and AURKA. In particular, CDK1 and CDK2 were suggested to be inactivated by LAT1 inhibition in all four cell lines. They may be principal key regulators of signaling networks altered in LAT1-inhibited cells. Furthermore, Western blot validated the decreased phosphorylation of CDK1/CDK2 substrates: Ser-807/811 of Rb, Ser-54 of Cdc6, and Ser-1213 of TOP2A (Figure 6B). Phosphorylation of these sites was reported to play important roles in the progression of cell cycle,⁵⁵⁻⁶¹ which suggests that such phosphorylation changes might induce the growth arrest caused by LAT1 inhibition. Cell cycle assay by flow cytometric analysis showed that JPH203 treatment induces G0/G1 phase arrest (Figure 6C).

We showed the potential of combination of LAT1 inhibitor with cell cycle-related kinase inhibitor for cancer treatment (Figure 7). We evaluated the combinations of JPH203 with five cell cycle-related kinase inhibitors whose targets were implicated to be inactivated by LAT1 inhibition in our phosphoproteomics. These drug combinations significantly reduced cell proliferation, especially dinaciclib and AT7519. Interestingly, dinaciclib and AT7519 target CDK1 and CDK2 which were implied to be key kinases in all four cell lines in our phosphoproteomics (Figure 6A). All tested inhibitors are FDA-approved or in clinical trials for cancers. Our study could suggest new possible indications of these drugs used in combinations for cancer therapy. CDK inhibitors with various specificity ranges have been developed recently,⁶² which would provide wider possibility to obtain more prominent anticancer effects in combination with LAT1 inhibitors.

Both proteomics and phosphoproteomics revealed a broad influence of LAT1 inhibition on various cellular processes other than cell cycle. Our phosphoproteomics indicated the activation of signaling pathways involved in actin cytoskeleton regulation. Previous phosphoproteomics study reported the upregulation of actin cytoskeleton regulatory pathways in drug-resistant cancer cells.⁶³ It would be interesting to examine whether the activation of actin cytoskeleton regulatory pathways is implicated in chemoresistance in LAT1-inhibited conditions. Furthermore, our study showed many possible regulators in LAT1-inhibited cells. Dozens of them were common among different cell lines, which include various types of molecules such as transcription regulator, kinase, and microRNA. They may be the regulatory components of networks perturbed by LAT1 inhibition and have clinical potential as new therapeutic targets in combination with LAT1 inhibitor for cancer therapy.

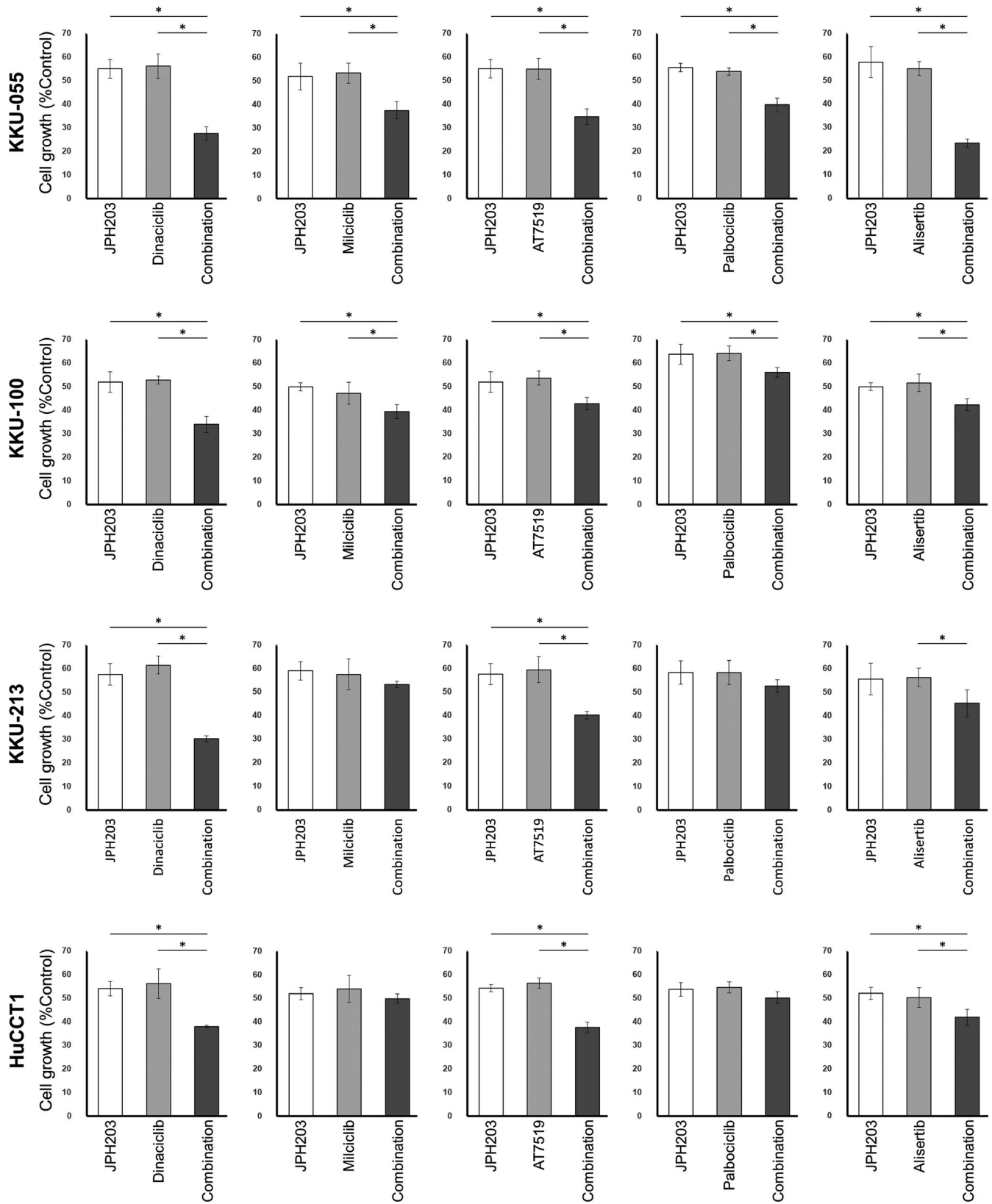


FIGURE 7 Effects of the combination of JPH203 with cell cycle-related kinase inhibitors, dinaciclib, miliciclib, AT7519, palbociclib, and alisertib. Biliary tract cancer (BTC) cell lines were treated with JPH203 or each cell cycle-related kinase inhibitor alone, or in combination. The concentrations of inhibitors used are described in Document S1. The significance of the difference between the treatments with each inhibitor alone and the combination was determined by one-way ANOVA followed by Tukey's multiple comparison test. Data represent means \pm SD ($n = 4$). *Tukey post hoc P -value $< .05$

Transcriptional regulator ATF4 was shown as one of the possible regulators activated by LAT1 inhibition in all four cell lines. This is consistent with previous reports indicating that the inhibition of LAT1 by JPH203 induces ATF4 expression.^{22,64} Recently, several studies have shown that ATF4 mediates the upregulation of amino acid transporters such as LAT1,⁶⁵ 4F2hc,⁶⁶ xCT,⁶⁷ ASCT1,⁶⁶ ASCT2,⁶⁶ CAT-1,⁶⁸ and SNAT2.⁶⁹ We, therefore, checked whether the expression of amino acid transporters was altered by LAT1 inhibition. Among 19 amino acid transporters identified in this study, nearly half of them were upregulated by JPH203. The upregulation of most of these amino acid transporters were previously reported to be mediated by ATF4. The upregulation of these transporters can influence amino acid balance in cancer cells. Moreover, our proteomics showed the upregulation of the tRNA charging pathway, which includes aminoacyl-tRNA synthetases. Aminoacyl-tRNA synthetases catalyze the ligation of corresponding amino acids to the cognate tRNAs and also function as amino acid sensors.^{70–73} Therefore, our results suggest that LAT1 inhibition causes an imbalance of intracellular amino acids not only through inhibition of its amino acid transport activity but also by upregulation of other amino acid transporters and aminoacyl-tRNA synthetases. The perturbations of intracellular amino acids by LAT1 inhibition can be complicated, which may be the reason why the downregulation of mTOR signaling by LAT1 inhibition was not detected in our phosphoproteomics even though leucine, a substrate of LAT1, stimulates mTORC1.²¹ To date, how LAT1 inhibition perturbs amino acid concentrations in cancer cells remains unknown and will be the focus of future studies. Furthermore, further studies are needed to reveal the amino acid signaling mechanisms leading to cell cycle arrest through CDK inhibition advocated in this study. An increase of G0/G1 phase population was found by JPH203 treatment (Figure 6C), while mTOR inactivation was not detected. There might be mechanisms other than those for G1 phase arrest induced by mTOR inhibitor such as rapamycin. In addition, our proteomics showed expression changes in many proteins in LAT1-inhibited cells, which is reasonable because a single amino acid, leucine, starvation reportedly leads to expression changes in approximately 700 genes,⁷⁴ and JPH203 treatment inhibits uptake of LAT1 substrates including leucine. However, it should be noted that the changes shown by our proteomics may include those caused by off-target effects of JPH203, which may provide clues to discover possible side effects in its clinical usage in further study.

In summary, we conducted proteomics and phosphoproteomics to determine biological pathways and phosphorylation cascades associated with anticancer effects of LAT1 inhibition. We revealed possible regulators and key kinases in LAT1-inhibited BTC cells, which include many cell cycle-related proteins and kinases. Among them, inactivation of CDKs was notable, especially CDK1 and CDK2. Interestingly, JPH203 treatment induced cell cycle arrest at G0/G1 phase. Furthermore, we found significant reduction of proliferation of BTC cells by combination of LAT1 inhibitor and cell cycle-related kinase inhibitor, which indicates the potential of new therapeutic strategies using LAT1 inhibitors for cancers. This study provides a

resource for future studies addressing the mechanisms of anticancer effects by LAT1 inhibition.

ACKNOWLEDGMENTS

This work was supported by the Japan Society for the Promotion of Science, Grant-in-Aid for Early-Career Scientists 19K16743 (to HO), for Scientific Research 19H03407 (to YK), for Challenging Research (Exploratory) 18K19429 (to YK), and by the Japan Agency for Medical Research and Development, the Project for Cancer Research And Therapeutic Evolution JP19cm0106151 and JP20cm0106151 (to YK), and by Collaborative Research Grant from J-Pharma Co., Ltd. KKKU-055, KKKU-100, and KKKU-213 cell lines were established by Dr. Banchob Spira. We thank Dr. Ryohei Narumi (National Institutes of Biomedical Innovation, Health and Nutrition) for advice on experimental design.

DISCLOSURE

YK received collaborative research grant from J-Pharma Co., Ltd. HE owns the shares of J-Pharma Co., Ltd. Other authors declare no conflicts of interest.

ORCID

Yoshikatsu Kanai  <https://orcid.org/0000-0001-8126-286X>

REFERENCES

- Pavlova NN, Thompson CB. The emerging hallmarks of cancer metabolism. *Cell Metab.* 2016;23:27–47.
- Hanahan D, Weinberg RA. Hallmarks of cancer: the next generation. *Cell.* 2011;144:646–674.
- Hosios A, Hecht V, Danai L, et al. Amino acids rather than glucose account for the majority of cell mass in proliferating mammalian cells. *Dev Cell.* 2016;36:540–549.
- Salisbury TB, Arthur S. The regulation and function of the L-type amino acid transporter 1 (LAT1) in cancer. *Int J Mol Sci.* 2018;19:2373.
- Kilberg MS, Shan J, Su N. ATF4-dependent transcription mediates signaling of amino acid limitation. *Trends Endocrinol Metab.* 2009;20:436–443.
- Nie C, He T, Zhang W, Zhang G, Ma X. Branched chain amino acids: beyond nutrition metabolism. *Int J Mol Sci.* 2018;19:954.
- Zhuang Y, Wang XX, He J, He S, Yin Y. Recent advances in understanding of amino acid signaling to mTORC1 activation. *Front Biosci.* 2019;24:971–982.
- Wang Q, Holst J. L-type amino acid transport and cancer: targeting the mTORC1 pathway to inhibit neoplasia. *Am J Cancer Res.* 2015;5:1281–1294.
- Kanai Y, Segawa H, Miyamoto KI, Uchino H, Takeda E, Endou H. Expression cloning and characterization of a transporter for large neutral amino acids activated by the heavy chain of 4F2 antigen (CD98). *J Biol Chem.* 1998;273:23629–23632.
- Kandasamy P, Gyimesi G, Kanai Y, Hediger MA. Amino acid transporters revisited: new views in health and disease. *Trends Biochem Sci.* 2018;43:752–789.
- Yanagida O, Kanai Y, Chairoungdua A, et al. Human L-type amino acid transporter 1 (LAT1): characterization of function and expression in tumor cell lines. *Biochim Biophys Acta Biomembr.* 2001;1514:291–302.
- Kobayashi H, Ishii Y, Takayama T. Expression of L-type amino acid transporter 1 (LAT1) in esophageal carcinoma. *J Surg Oncol.* 2005;90:233–238.

13. Nawashiro H, Otani N, Shinomiya N, et al. L-type amino acid transporter 1 as a potential molecular target in human astrocytic tumors. *Int J cancer*. 2006;119:484–492.
14. Kaira K, Oriuchi N, Imai H, et al. L-type amino acid transporter 1 and CD98 expression in primary and metastatic sites of human neoplasms. *Cancer Sci*. 2008;99:2380–2386.
15. Sakata T, Ferdous G, Tsuruta T, et al. L-type amino-acid transporter 1 as a novel biomarker for high-grade malignancy in prostate cancer. *Pathol Int*. 2009;59:7–18.
16. Ichinoe M, Mikami T, Yoshida T, et al. High expression of L-type amino-acid transporter 1 (LAT1) in gastric carcinomas: comparison with non-cancerous lesions. *Pathol Int*. 2011;61:281–289.
17. Furuya M, Horiguchi J, Nakajima H, Kanai Y, Oyama T. Correlation of L-type amino acid transporter 1 and CD98 expression with triple negative breast cancer prognosis. *Cancer Sci*. 2012;103:382–389.
18. Kaira K, Kawashima O, Endoh H, et al. Expression of amino acid transporter (LAT1 and 4F2hc) in pulmonary pleomorphic carcinoma. *Hum Pathol*. 2019;84:142–149.
19. Fuchs BC, Bode BP. Amino acid transporters ASCT2 and LAT1 in cancer: Partners in crime? *Semin Cancer Biol*. 2005;15:254–266.
20. Scalise M, Pochini L, Galluccio M, Console L, Indiveri C. Glutamine transport and mitochondrial metabolism in cancer cell growth. *Front Oncol*. 2017;7:306.
21. Saxton RA, Sabatini DM. mTOR signaling in growth, metabolism, and disease. *Cell*. 2017;168:960–976.
22. Rosilio C, Nebout M, Imbert V, et al. L-type amino-acid transporter 1 (LAT1): A therapeutic target supporting growth and survival of T-cell lymphoblastic lymphoma/T-cell acute lymphoblastic leukemia. *Leukemia*. 2015;29:1253–1266.
23. Häfliger P, Graff J, Rubin M, et al. The LAT1 inhibitor JPH203 reduces growth of thyroid carcinoma in a fully immunocompetent mouse model. *J Exp Clin Cancer Res*. 2018;37:234.
24. Cormerais Y, Pagnuzzi-Boncompagni M, Schrötter S, et al. Inhibition of the amino-acid transporter LAT1 demonstrates anti-neoplastic activity in medulloblastoma. *J Cell Mol Med*. 2019;23:2711–2718.
25. Yue M, Jiang J, Gao P, Liu H, Qing G. Oncogenic MYC activates a feedforward regulatory loop promoting essential amino acid metabolism and tumorigenesis. *Cell Rep*. 2017;21:3819–3832.
26. Dann SG, Ryskin M, Barsotti AM, et al. Reciprocal regulation of amino acid import and epigenetic state through Lat1 and EZH 2. *EMBO J*. 2015;34:1773–1785.
27. Oda K, Hosoda N, Endo H, et al. L-Type amino acid transporter 1 inhibitors inhibit tumor cell growth. *Cancer Sci*. 2010;101:173–179.
28. Yun D-W, Lee SA, Park M-G, et al. JPH203, an L-type amino acid transporter 1-selective compound, induces apoptosis of YD-38 human oral cancer cells. *J Pharmacol Sci*. 2014;124:208–217.
29. Hayashi K, Jutabha P, Maeda S, et al. LAT1 acts as a crucial transporter of amino acids in human thymic carcinoma cells. *J Pharmacol Sci*. 2016;132:201–204.
30. Yothaisong S, Dokduang H, Anzai N, et al. Inhibition of l-type amino acid transporter 1 activity as a new therapeutic target for cholangiocarcinoma treatment. *Tumor Biol*. 2017;39:1010428317694545.
31. Enomoto K, Sato F, Tamagawa S, et al. A novel therapeutic approach for anaplastic thyroid cancer through inhibition of LAT1. *Sci Rep*. 2019;9:14616.
32. Higuchi K, Sakamoto S, Ando K, et al. Characterization of the expression of LAT1 as a prognostic indicator and a therapeutic target in renal cell carcinoma. *Sci Rep*. 2019;9:16776.
33. Maimaiti M, Sakamoto S, Yamada Y, et al. Expression of L-type amino acid transporter 1 as a molecular target for prognostic and therapeutic indicators in bladder carcinoma. *Sci Rep*. 2020;10:1292.
34. Watabe T, Ikeda H, Nagamori S, et al. 18F-FBPA as a tumor-specific probe of L-type amino acid transporter 1 (LAT1): a comparison study with 18F-FDG and 11C-Methionine PET. *Eur J Nucl Med Mol Imaging*. 2017;44:321–331.
35. Aoki M, Watabe T, Nagamori S, et al. Distribution of LAT1-targeting PET tracer was independent of the tumor blood flow in rat xenograft models of C6 glioma and MIA PaCa-2. *Ann Nucl Med*. 2019;33:394–403.
36. Nakanishi K, Ogata S, Matsuo H, et al. Expression of LAT1 predicts risk of progression of transitional cell carcinoma of the upper urinary tract. *Virchows Arch*. 2007;451:681–690.
37. Kaira K, Oriuchi N, Imai H, et al. Prognostic significance of L-type amino acid transporter 1 expression in resectable stage I-III nonsmall cell lung cancer. *Br J Cancer*. 2008;98:742–748.
38. Kaira K, Sunose Y, Arakawa K, et al. Prognostic significance of L-type amino-acid transporter 1 expression in surgically resected pancreatic cancer. *Br J Cancer*. 2012;107:632–638.
39. Kaira K, Sunose Y, Ohshima Y, et al. Clinical significance of L-type amino acid transporter 1 expression as a prognostic marker and potential of new targeting therapy in biliary tract cancer. *BMC Cancer*. 2013;13:482.
40. Toyoda M, Kaira K, Ohshima Y, et al. Prognostic significance of amino-acid transporter expression (LAT1, ASCT2, and xCT) in surgically resected tongue cancer. *Br J Cancer*. 2014;110:2506–2513.
41. Ogawa H, Kaira K, Motegi Y, et al. Role of amino acid transporter expression as a prognostic marker in patients with surgically resected colorectal cancer. *Anticancer Res*. 2019;39:2535–2543.
42. Watabe T, Kaneda-Nakashima K, Shirakami Y, et al. Targeted alpha therapy using astatine (211At)-labeled phenylalanine: a preclinical study in glioma bearing mice. *Oncotarget*. 2020;11:1388–1398.
43. Shennan DB, Thomson J. Inhibition of system L (LAT1/CD98hc) reduces the growth of cultured human breast cancer cells. *Oncol Rep*. 2008;20:885–889.
44. Ohshima Y, Kaira K, Yamaguchi A, et al. Efficacy of system I amino acid transporter 1 inhibition as a therapeutic target in esophageal squamous cell carcinoma. *Cancer Sci*. 2016;107:1499–1505.
45. Jutabha M, Kumar V, Fisher J, et al. Developing selective L-amino acid transport 1 (LAT1) inhibitors: a structure-activity relationship overview. *Med Res Arch*. 2019;7. <https://doi.org/10.18103/mra.v7i12.2014>.
46. Okano N, Naruge D, Kawai K, et al. First-in-human phase I study of JPH203, an L-type amino acid transporter 1 inhibitor, in patients with advanced solid tumors. *Invest New Drugs*. 2020;38(5):1495–1506.
47. Boulos JC, Yousof Idres MR, Efferth T. Investigation of cancer drug resistance mechanisms by phosphoproteomics. *Pharmacol Res*. 2020;160:105091.
48. Jung JH, You S, Oh JW, et al. Integrated proteomic and phosphoproteomic analyses of cisplatin-sensitive and resistant bladder cancer cells reveal CDK2 network as a key therapeutic target. *Cancer Lett*. 2018;437:1–12.
49. Masuda T, Tomita M, Ishihama Y. Phase transfer surfactant-aided trypsin digestion for membrane proteome analysis. *J Proteome Res*. 2008;7:731–740.
50. Narumi R, Tomonaga T. Quantitative analysis of tissue samples by combining itraq isobaric labeling with selected/multiple reaction monitoring (SRM/MRM). *Methods Mol Biol*. 2016;1355:85–101.
51. Rappsilber J, Ishihama Y, Mann M. Stop and go extraction tips for matrix-assisted laser desorption/ionization, nanoelectrospray, and LC/MS sample pretreatment in proteomics. *Anal Chem*. 2003;75:663–670.
52. Pascovici D, Handler DCL, Wu JX, Haynes PA. Multiple testing corrections in quantitative proteomics: a useful but blunt tool. *Proteomics*. 2016;16:2448–2453.
53. Casado P, Rodriguez-Prados J-C, Cosulich SC, et al. Kinase-substrate enrichment analysis provides insights into the heterogeneity of signaling pathway activation in leukemia cells. *Sci Signal*. 2013;6:rs6.
54. Wiredja DD, Koyutürk M, Chance MR. The KSEA App: a web-based tool for kinase activity inference from quantitative phosphoproteomics. *Bioinformatics*. 2017;33:3489–3491.

55. Hu QJ, Lees JA, Buchkovich KJ, Harlow E. The retinoblastoma protein physically associates with the human cdc2 kinase. *Mol Cell Biol.* 1992;12:971–980.
56. Mailand N, Diffley JFX. CDKs promote DNA replication origin licensing in human cells by protecting Cdc6 from APC/C-dependent proteolysis. *Cell.* 2005;122:915–926.
57. Duursma AM, Agami R. CDK-dependent stabilization of Cdc6: linking growth and stress signals to activation of DNA replication. *Cell Cycle.* 2005;4:1725–1728.
58. Sanidas I, Morris R, Fella KA, et al. A code of mono-phosphorylation modulates the function of RB. *Mol Cell.* 2019;73:985–1000.e6.
59. Wells NJ, Hickson ID. Human topoisomerase II alpha is phosphorylated in a cell-cycle phase-dependent manner by a proline-directed kinase. *Eur J Biochem.* 1995;231:491–497.
60. Ishida R, Takashima R, Koujin T, et al. Mitotic specific phosphorylation of serine-1212 in human DNA topoisomerase II α . *Cell Struct Funct.* 2001;26:215–226.
61. Xu YX, Manley JL. The prolyl isomerase Pin1 functions in mitotic chromosome condensation. *Mol Cell.* 2007;26:287–300.
62. Sánchez-Martínez C, Gelbert LM, Lallena MJ, De Dios A. Cyclin dependent kinase (CDK) inhibitors as anticancer drugs. *Bioorganic Med Chem Lett.* 2015;25:3420–3435.
63. Vyse S, McCarthy F, Broncel M, et al. Quantitative phosphoproteomic analysis of acquired cancer drug resistance to pazopanib and dasatinib. *J Proteomics.* 2018;170:130–140.
64. Cormerais Y, Giuliano S, LeFloch R, et al. Genetic disruption of the multifunctional CD98/LAT1 complex demonstrates the key role of essential amino acid transport in the control of mTORC1 and tumor growth. *Cancer Res.* 2016;76:4481–4492.
65. Chen R, Zou Y, Mao D, et al. The general amino acid control pathway regulates mTOR and autophagy during serum/glutamine starvation. *J Cell Biol.* 2014;206:173–182.
66. Wang Q, Tiffen J, Bailey CG, et al. Targeting amino acid transport in metastatic castration-resistant prostate cancer: effects on cell cycle, cell growth, and tumor development. *J Natl Cancer Inst.* 2013;105:1463–1473.
67. Ye P, Mimura J, Okada T, et al. Nrf2- and ATF4-dependent upregulation of xCT modulates the sensitivity of T24 bladder carcinoma cells to proteasome inhibition. *Mol Cell Biol.* 2014;34:3421–3434.
68. Lopez A, Wang C, Huang C, et al. A feedback transcriptional mechanism controls the level of the arginine/lysine transporter cat-1 during amino acid starvation. *Biochem J.* 2007;402:163–173.
69. Pali SS, Thiaville MM, Pan YX, Zhong C, Kilberg MS. Characterization of the amino acid response element within the human sodium-coupled neutral amino acid transporter 2 (SNAT2) System A transporter gene. *Biochem J.* 2006;395:517–527.
70. Ko Y-G, Kim E-K, Kim T, et al. Glutamine-dependent antiapoptotic interaction of human glutaminyl-tRNA synthetase with apoptosis signal-regulating kinase 1. *J Biol Chem.* 2001;276:6030–6036.
71. Han JM, Jeong SJ, Park MC, et al. Leucyl-tRNA synthetase is an intracellular leucine sensor for the mTORC1-signaling pathway. *Cell.* 2012;149:410–424.
72. Yoon MS, Son K, Arauz E, Han JM, Kim S, Chen J. Leucyl-tRNA synthetase activates Vps34 in amino acid-sensing mTORC1 signaling. *Cell Rep.* 2016;16:1510–1517.
73. Di HX, Gong W, Zhang JN, et al. Sensing and transmitting intracellular amino acid signals through reversible lysine aminoacylations. *Cell Metab.* 2018;27:151–166.e6.
74. Deval C, Chaveroux C, Maurin AC, et al. Amino acid limitation regulates the expression of genes involved in several specific biological processes through GCN2-dependent and GCN2-independent pathways. *FEBS J.* 2009;276:707–718.

SUPPORTING INFORMATION

Additional supporting information may be found online in the Supporting Information section.

How to cite this article: Okanishi H, Ohgaki R, Okuda S, Endou H, Kanai Y. Proteomics and phosphoproteomics reveal key regulators associated with cytostatic effect of amino acid transporter LAT1 inhibitor. *Cancer Sci.* 2021;112:871–883. <https://doi.org/10.1111/cas.14756>